PROOF COPY 049312RSI

Experimental study of nanoparticle detection by optical gradient forces

Filipp V. Ignatovich and Lukas Novotny[a)]
The Institute of Optics, University of Rochester, Rochester, New York 14627

(Received 24 June 2003; accepted 18 September 2003)

We experimentally investigate a novel particle detection scheme that makes use of optical gradient forces. The path of nanoscale particles carried in a microfluidic channel is perturbed by a strongly focused laser beam. The perturbation is interferometrically recorded with a quadrant detector and the temporal asymmetry of the detector signal yields information about the force exerted on the particles by the laser focus. Large particles experience strong forces, thus rendering a highly asymmetric signal whereas small particles pass the laser focus almost unperturbed thus rendering a symmetric signal. We analyze the influence of experimental parameters such as laser power and fluid speed on the precision of the method and discuss the influence of Brownian motion. © *2003 American Institute of Physics.* [DOI: 10.1063/1.1628823]

PROOF COPY 049312RSI

I. INTRODUCTION

With the advent of nanoscience and nanotechnology it becomes increasingly important to reliably assess the size of nanometer scale particles. The detection of nanoparticles is also important in many areas of modern society, such as public health, public safety, and strategic planning. For example, inhalation of ultrafine particles that originate from emissions of various kinds can be deposited in the upper respiratory system and may aggravate symptoms of rhinitis and allergies.[1,2] There is also an increasing demand for sensors that detect the presence of warfare and other harmful biological agents in public areas or in field conditions, due to the increased threat of bioterrorism.[3,4]

Most commonly, *optical* methods for particle detection rely on light scattering.[5] In the simplest version, these so-called optical particle counters (OPCs)[6,7] consist of a light source (usually a laser) which illuminates a sample volume of an aerosol or liquid flow containing the particles of interest. An off-axis detector collects the scattered light. The latter is a function of particle properties such as the size, concentration, and optical density. There are many variations of OPCs, some of which count individual particles, such as the flow cytometer,[8] the phase Doppler anemometer (PDA),[9] and some versions of condensation nuclei counters.[10] Other OPCs measure ensemble averages. Some examples are dynamic light scattering,[11] nephelometers (or multiangle photometers),[12] and other versions of condensation nuclei counter.[10]

Light scattering measurements depend very strongly on the particle size (sixth power). This strong size dependence makes the smallest particles difficult to detect, that is, the scattered signal is weak and often cannot be extracted from background noise. Therefore, new detection schemes are necessary for recognition of ultrasmall particles.

The invention of optical tweezers[13,14] made it possible to manipulate matter with forces in the pico-Newton range.[15] The force is generated by the field gradient near a tightly focused laser beam. For dielectric materials, the force is directed towards the center of focus, thereby preventing a trapped object from escaping. In particles much smaller than the wavelength of the trapping laser the force acting on a spherical particle is given by

$$\mathbf{F}=2\pi R^3\epsilon_0\epsilon_s\frac{\epsilon_p-\epsilon_s}{\epsilon_p+2\epsilon_s}\nabla|\mathbf{E}(\mathbf{r}_0)|^2, \tag{1}$$

where ϵ_p is the dielectric permittivity of the particle, ϵ_s is the dielectric permittivity of the environment (water, air, vacuum), $\mathbf{E}(\mathbf{r}_0)$ is the complex electric field vector at the origin, $\mathbf{r}_0$, of the particle, and R is the particle radius. Unlike light scattering, the gradient force $\mathbf{F}$ scales with the third power of the particle size (R^3 vs R^6). Therefore, it is intuitive to apply gradient forces for the detection of subwavelength sized particles.[16]

Let us assume that the gradient force acting on a particle passing through a laser focus is sufficiently strong to perturb motion of the particle without trapping it. This perturbation is stronger the larger the particle is because of the R^3 dependence of the gradient force. If the particle is moving in a viscous medium it will also experience Stokes force proportional to the particle's velocity. As the particle approaches the laser focus, the optical gradient force acts along the Stokes force, and the particle accelerates towards the focus. However, as the particle crosses the center of the focused beam, the optical gradient force opposes the Stokes force, thus slowing the particle down. So because of the optical gradient force, the velocity trajectory of any particle will be nonuniform. While a small particle passes almost unperturbed, a larger particle is first pulled towards the focus and then slowly released.

Particle motion through the laser focus can be monitored using a quadrant detector. The essence of the detection is as follows: the transmitted light and the light scattered by a particle create an interference pattern on the detector, which shifts as the particle moves through the focus. The difference in signal between two opposing halves of the detector provides information about the magnitude of the shift and thus

a)Electronic mail: novotny@optics.rochester.edu

 © 2003 American Institute of Physics

PROOF COPY 049312RSI

PROOF COPY 049312RSI

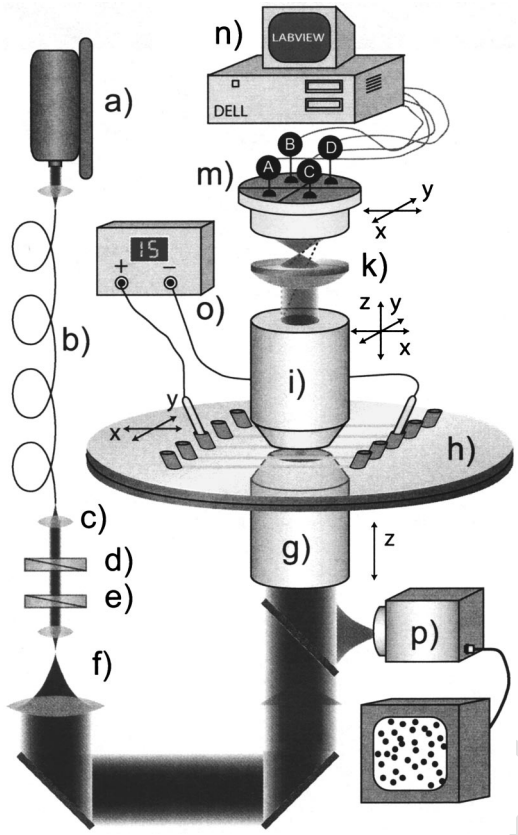

FIG. 1. Experimental setup. The light from a 532 nm laser (a) is transmitted through an optical fiber (b), collimated (c), and polarized by using a λ/4 wave plate (d) and a λ/2 wave plate (e). The beam is expanded (f) and focused with a NA=1.4 objective (g) into the flow cell (h). The transmitted and scattered light is collected with a NA=0.8 objective (i). The interference pattern at the back aperture of the collecting objective is imaged (k) onto a quadrant detector (m). A data acquisition board (n) is used to read and process the detector signal. The fluid in the flow cell is controlled by electroosmosis (o) and a CCD camera (p) is used to image the backscattered light.

the position of the particle relative to the focus. More details about the employed interferometric detection method can be found in Refs. 16–19.

We have recently demonstrated that the temporal profile of the detector signal reflects the optical gradient force which acts on a particle during its motion through the focus.[16] In the present article we provide experimental proof of this novel particle detection scheme and we demonstrate successful detection and separation of a mixture of particles with radii $R=50$ and 100 nm.

II. EXPERIMENTAL SETUP

A. Optical system

The experimental setup is shown in Fig. 1. After passing through a single-mode fiber, light from a 532 nm laser (Coherent Inc., Santa Clara, CA) is first collimated and then passed through λ/4 and λ/2 wave plates to obtain linear polarization.

The beam was expanded and sent into an inverted microscope (TE300, Nikon, Japan). A high numerical aperture (NA) objective (NA=1.4, PlanApo, 60×) is used to tightly focus the laser beam into a flow cell. The transmitted beam and the light scattered from particles in the flow cell are collected by a 0.85 NA objective. The interference of these two fields is imaged with a lens onto a quadrant detector (SPOT 9DMI, UDT Sensors, Hawthorne, CA).

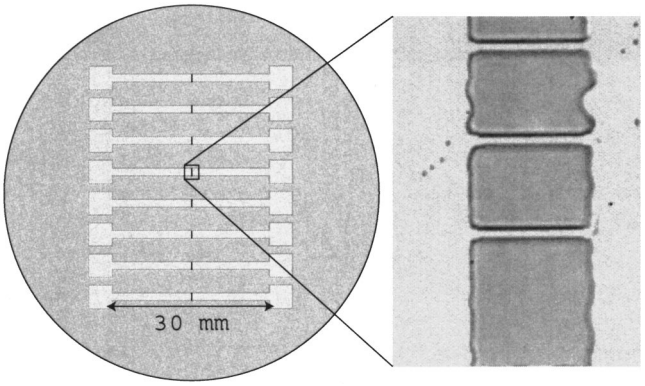

FIG. 2. (a) Wafer consisting of eight separate flow cells (depth of 500 nm) fabricated between pairs of reservoirs (separated by 30 mm). In the center, each flow cell comprises a barrier with 500 nm wide nanochannels. (b) Optical micrograph showing the barrier and the nanochannels together with $R=100$ nm particles.

In order to prevent large particles from being trapped and thus blocking the laser focus we have previously developed a feedback system that automatically attenuates the laser power when the backscattered light exceeds a given threshold.[16] In this work, the feedback is deactivated because only solutions with small particles are used.

B. Flow cell

In a flow cell with dimensions considerably larger than the laser focus, large particles passing at some distance from the focus will experience the same force as small particles passing right through the focus. In order to eliminate this uncertainty, we have fabricated an array of nanochannels with width and depth of only 500 nm. The 15 μm long nanochannels connect to an array of larger flow cells between a pair of reservoirs separated by 30 mm (Fig. 2).

The flow cells were fabricated at the Cornell Nanofabrication Facility. Two borosilicate glass wafers (Schott Glass, Germany) were precleaned for 20 min in RCA1 solution (one part 27% ammonium hydroxide, two parts 30% hydrogen peroxide, and three parts de-ionized water) at 70 °C, for 15 min. One wafer was spin coated with *i*-line photoresist (O*i*R 620-7*i*) at 3000 rpm for 30 s at a 3 s ramping speed. The nanosized parts of the flow cell were patterned using a 10× stepper (GCA Corp., Andover, MA), and the micron-sized features were patterned using the EV602 contact aligner (Electronic Visions, Phoenix, AZ). The channels were etched using the reactive ion etching technique. The remaining resist was then removed by soaking the wafer in the nanostrip solution (stabilized sulfuric acid) at 80 °C for 10 min. A second glass wafer was used to seal the channels. Holes for liquid delivery were made in the second wafer using a sandblasting tool. The two wafers were cleaned in RCA1 solution again and then bonded together under 2000 N pressure at 550 °C for 10 h. Later, plastic reservoirs were glued on top of the second wafer (see Fig. 1), and covered

PROOF COPY 049312RSI

PROOF COPY 049312RSI

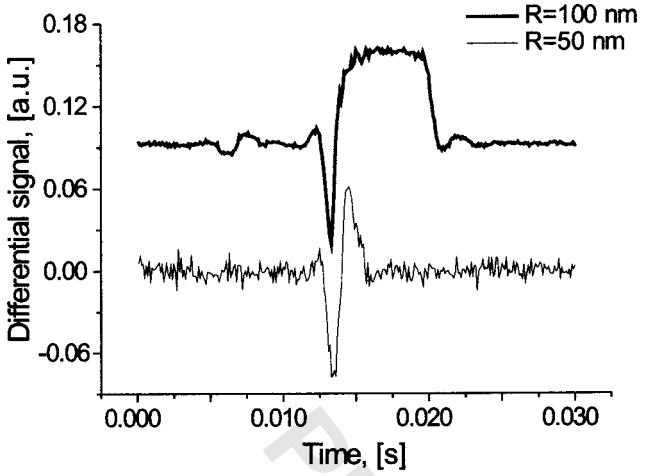

FIG. 3. Detector signal for a $R=100$ nm particle (top curve) and a $R=50$ nm particle (bottom curve) passing through the laser focus. The left halves of the curves originate from particle movement toward the focus, and the right halves correspond to particles leaving the focus. The asymmetry of the curves (width of dip vs width of peak) reflects the nonuniform velocity profile induced by the optical gradient force. The ratio between the widths of the peak and the dip is defined as the force parameter.

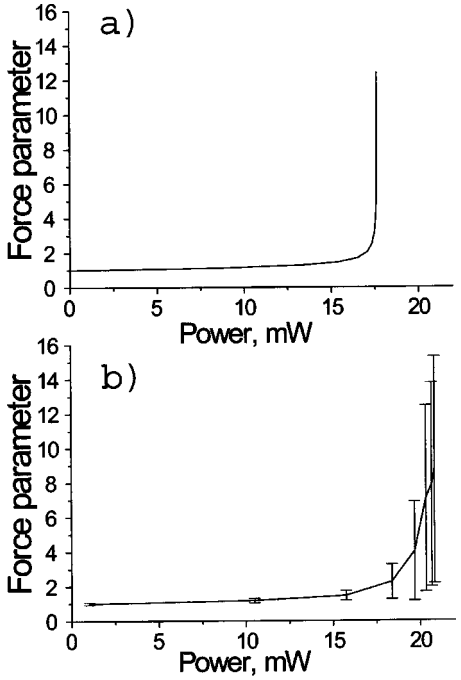

FIG. 4. (a) Numerical calculation of the force parameter vs the laser power in the absence of Brownian motion for $R=100$ nm particles in water moving at 1 mm/s. There is a clear distinction between trapping ($P>17.5$ mW) and perturbed motion ($P<17.5$ mW). (b) Force parameter vs the laser power in the presence of simulated Brownian motion. The time a particle spends in the trap varies, and the error bars show standard deviation of this variation.

with ''parafilm'' foil in order to prevent dust from entering the reservoirs. Each wafer assembly contains 8 separate flow cells, each with 65 nanochannels.

Factory prepared bead solutions (polystyrene, $R=50$ and 100 nm, Polysciences Inc., Warrington, PA) were diluted by adding de-ionized water to achieve the desired particle concentrations (approx 10^{10} particles/ml) and then mixed together. Tween-20 surfactant (0.02% by volume) was added to the solution to prevent the particles from clustering. The solution was then sonicated for 20 min prior to filling the reservoirs.

In order to induce and control liquid flow in the nanochannels, two gold electrodes were dipped into a pair of reservoirs and voltage was applied. The liquid is pumped from one reservoir to the other by electro-osmosis.[20] A 10 V potential between the two reservoirs resulted in fluid flow in the nanochannels of ≈ 500 μm/s. This estimate was calculated by measuring the time it takes for a particle to pass the focus with diameter given by $0.82\lambda/\mathrm{NA}$ and by monitoring individual particle trajectories with a charge coupled device (CCD) and a monitor.

The size of the laser focus can be estimated from the laser wavelength ($\lambda=532$ nm) and the numerical aperture of the objective ($\mathrm{NA}=1.4$) to be $0.82\lambda/\mathrm{NA}\approx 310$ nm which is less than the diameter of the fabricated nanochannels. Even though flow outside the nanochannels is driven by electro-osmosis, flow inside the nanochannels is pressure induced. This is because the velocity profile of the liquid speed inside the nanochannels is much higher than the corresponding value defined by the voltage applied. Consequently, the velocity profile of the liquid is not uniform: in the center of the channel the liquid moves faster than near the walls of the channel. Therefore, particles are pulled towards the center of a nanochannel and pass through the laser focus.

C. Data analysis

The signal from each quadrant of the quadrant detector (A, B, C, and D in Fig. 1) is recorded at a rate of 10 kS/s using a NI-6052E data acquisition card and LabView software (National Instruments, Austin, TX). The normalized forward difference signal,

$$S=\frac{(C+D)-(A+B)}{A+B+C+D}, \tag{2}$$

is computed and analyzed.

Signal S, measured for a $R=100$ and a $R=50$ nm particle is shown in Fig. 3. Both curves are characterized by a dip followed by a peak. According to Eq. (1), the $R=100$ nm particle experiences stronger force, and hence stronger perturbation, than the $R=50$ nm particle. Consequently, the asymmetry of the signal (width of dip versus width of peak) is larger for the $R=100$ nm particle. As a measure of the gradient force experienced we define the *force parameter* as

$$\text{force parameter}=\frac{\text{width of peak}}{\text{width of dip}}. \tag{3}$$

The force parameter is equal to unity when the optical force is negligible, i.e., when a particle spends the same amount of time on either side of the focus. The force parameter grows as the force increases.

III. EXPERIMENTAL RESULTS

Brownian motion has a strong influence on the force parameter. Without Brownian motion, the detector signal can

PROOF COPY 049312RSI

PROOF COPY 049312RSI

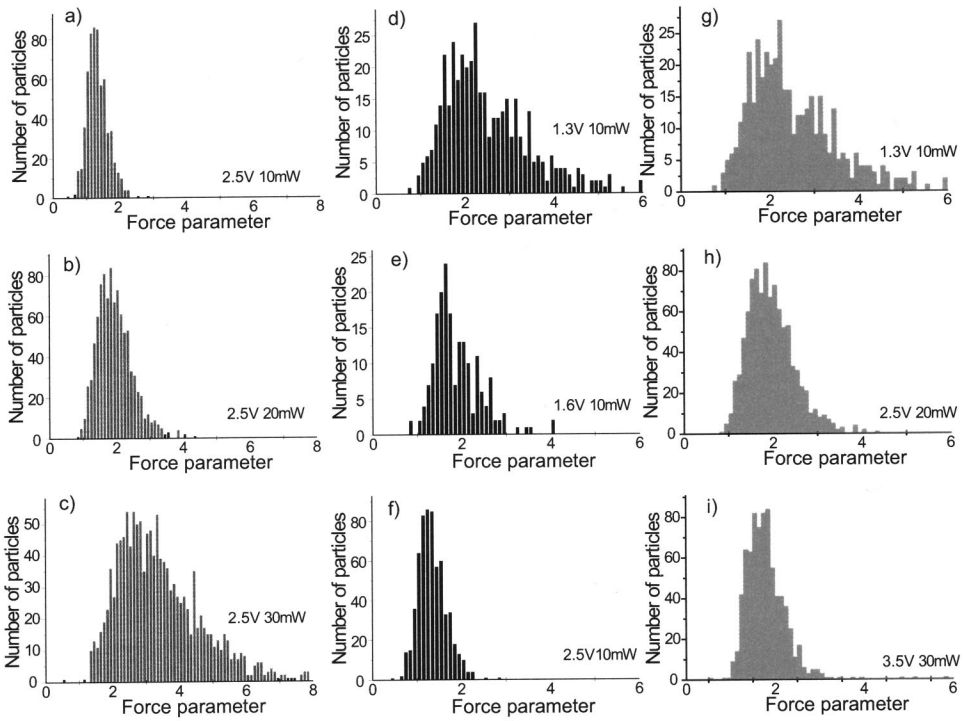

FIG. 5. Measurements of force parameter distributions for $R=100$ nm particles. The position and width of the distribution can be controlled by the laser power and speed of the liquid. (a)–(c) The liquid's speed is constant (voltage applied is 2.5 V) and the power is changed from 10 to 30 mW. Increasing the laser power shifts the distribution toward higher values. The distribution is simultaneously broadened because the particles spend more time in the laser focus. (d)–(f) The laser power is kept constant ($P=10$ mW) and the liquid's speed is changed by changing the voltage applied from 1.3 to 2.5 V. Increasing the liquid's speed narrows the distribution, however the distribution is shifted toward lower values because the strength of the optical gradient force is reduced in comparison to the Stokes force. Laser power and liquid speed are increased: (g) $P=10$ mW and the voltage is 1.3 V; (h) $P=20$ mW, voltage is 2.5 V; (i) $P=30$ mW, voltage is 3.5 V. The position of the distribution remains unaffected whereas the width decreases.

be assigned to a particular particle trajectory; a particle that is strongly perturbed can be clearly distinguished from a particle that is trapped [Fig. 4(a)]. However, when Brownian motion is taken into account, this distinction becomes difficult since the particle trajectory can be considered as being composed of many short trapping events. Within the limit when the gradient force is much smaller than the Stokes force, the trapping time is negligible and motion of the particle is unperturbed. Conversely, when the optical force is much stronger than the Stokes force, the trapping time is larger than the duration of the experiment and the particle is trapped in a stable potential. In the intermediate situation, i.e., when the gradient force is comparable to the Stokes force, the particle gets trapped for only a short period of time. In this case, the trapping time is strongly influenced by Brownian motion and identical particles yield different trajectories. As a result, the force parameter for particles of the same size is distributed over some range. In order to distinguish differently sized particles one has to ensure that the corresponding distributions are sufficiently separated.

The mean value of the force parameter distribution depends strongly on the particle size. For very small particles it is centered near unity (small optical force) and for larger particles it is centered at larger values. For a clear distinction between two particle sizes it is necessary to achieve a large separation between the two distributions. This can be achieved by adjusting two experimental parameters: the speed of the liquid and the laser power (Stokes force and optical force, respectively).

The laser power defines the strength of the optical force that acts on a particle. As shown in Figs. 5(a)–5(c), the force parameter distribution can be shifted toward higher values by increasing the laser power. However, as the distribution shifts toward higher values, the width of the distribution increases. The stronger the force gradient, the longer the time a particle spends in the laser focus and the more sensitive it becomes to Brownian motion.

Increasing the speed of the liquid reduces the time a particle spends in the focus and lowers the effect of Brownian motion. Consequently, the width of the force parameter distribution decreases, as can be seen in Figs. 5(d)–5(f). However, the center of the distribution is also influenced by the velocity of the particles. As the velocity increases, the center of the force parameter shifts toward smaller values because large liquid speeds are associated with strong Stokes forces that reduce the influence of the optical force.

In order to maximize the separation between force parameter distributions, it is necessary to minimize the time a particle spends in the focus and to keep the optical force comparable to the Stokes force. As shown in Figs. 5(g)–5(i), the width of the force parameter distribution reduces while the mean value remains largely unaffected when the laser power and the liquid's speed are increased simultaneously.

To demonstrate the principle of operation of our nanoparticle detection scheme, a mixture of $R=100$ and 50 nm particles was added to the flow cell. The measured force parameter distribution is shown in Fig. 6. Two peaks can be

PROOF COPY 049312RSI

PROOF COPY 049312RSI

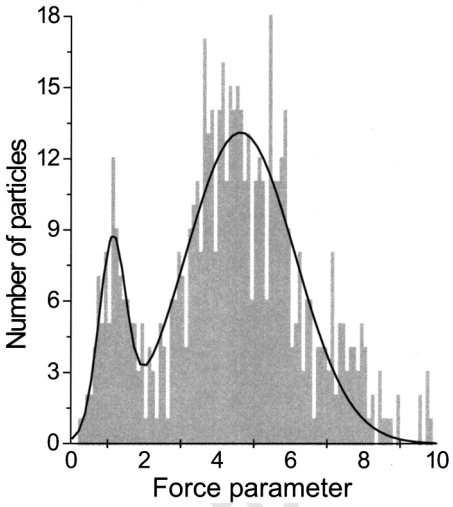

FIG. 6. Measurements of the force parameter distribution for a mixture of $R=50$ and 100 nm particles. The left peak corresponds to $R=50$ nm particles and the right peak to $R=100$ nm particles. The laser power is 60 mW and the electro-osmotic flow is driven by 15 V ($v\approx 0.9$ mm/s). The solid curve was added as a guide to the eye.

identified which correspond to $R=50$ nm particles (left peak) and $R=100$ nm particles (right peak).

The precision of the method presented is limited by Brownian motion. The precision can be improved by increasing the speed of the particles that pass through the focus (i.e., reducing the time a particle spends in the focus) and by increasing the laser power (i.e., increasing the perturbation of the particle). However, both power and speed are limited by several factors. Laser power is limited by heating of the medium and particles. The liquid's speed is limited by the pressure damage threshold for the nanochannels and by the detection bandwidth (higher liquid speeds require higher detection bandwidths to measure the particle trajectory; an increase in bandwidth results in higher noise which limits the lowest detectable size of particles). Nevertheless, the parameters can be optimized for recognition of particles of certain size.

ACKNOWLEDGMENTS

The authors wish to acknowledge stimulating discussions with their colleagues (A. Hartschuh, A. Bouhelier, and M. Beversluis). This work was funded by DARPA under Grant No. MDA972-00-1-0021. Nanochannel fabrication was done at the Cornell Nanofabrication Facility.

[1] A. Fernandez, J. O. L. Wendt, N. Wolski, K. R. G. Hein, S. J. Wang, and M. L. Witten, Chemosphere **51**, 1129 (2003).
[2] E. G. Barrett, K. Rudolph, L. E. Bowen, B. A. Muggenburg, and D. E. Bice, Inhalation Toxicol. **15**, 151 (2003).
[3] L. A. Broussard, Mol. Diagn. **6**, 323 (2001).
[4] M. R. Hillman, Vaccine **20**, 3055 (2002).
[5] C. F. Bohren and D. R. Huffman, *Absorption and Scattering of Light by Small Particles* (Wiley, New York, 1983).
[6] L. Fabiny, Opt. Photonics News **9**, 34 (1998).
[7] M. Kerker, Aerosol Sci. Technol. **27**, 522 (1997).
[8] A. L. Givan, *Flow Cytometry First Principles* (Wiley, New York, 2001).
[9] E. D. Hirleman, Part. Part. Syst. Charact. **13**, 59 (1996).
[10] P. H. McMurry, Aerosol Sci. Technol. **33**, 297 (2000).
[11] N. A. Clark, J. H. Lancek, and G. B. Benedek, Am. J. Phys. **38**, 575 (1970).
[12] J. Heintzenberg and R. J. Charlson, J. Atmos. Ocean. Technol. **13**, 987 (1996).
[13] A. Ashkin and J. P. Gordon, Opt. Lett. **8**, 511 (1983).
[14] A. Ashkin, J. M. Dziedzic, J. E. Bjorkholm, and S. Chu, Opt. Lett. **11**, 288 (1986).
[15] M. J. Lang and S. M. Block, Am. J. Phys. **71**, 201 (2003).
[16] F. V. Ignatovich, A. Hartschuh, and L. Novotny, J. Mod. Opt. **50**, 1509 (2003).
[17] D. R. Pettit and T. W. Peterson, U.S. Patent No. 4,477,187 (filed 1984); J. S. Batchelder and M. A. Taubenblatt, U.S. Patent No. 5,037,202 (filed 1991); J. S. Batchelder, D. M. DeCain, M. A. Taubenlatt, H. K. Wickramasinghe, and C. C. Williams, U.S. Patent No. 5,061,070 (filed 1991).
[18] J. S. Batchelder and M. A. Taunbenlatt, Appl. Phys. Lett. **55**, 215 (1989).
[19] F. Gittes and C. F. Schmidt, Opt. Lett. **23**, 7 (1998).
[20] *Electric Field Applications: In Chromatography, Industrial, and Chemical Processes*, edited by T. Tsuda (Winheim, New York, 1995).

PROOF COPY 049312RSI